Shi *et al. Energy Mater* 2023;3:300036
DOI: 10.20517/energymater.2023.27

Energy Materials

Article

Open Access

Check for updates

Nanostructured block copolymer single-ion conductors for low-temperature, high-voltage and fast charging lithium-metal batteries

Junli Shi[1], Huu-Dat Nguyen[2], Zhen Chen[3,4], Rui Wang[5], Dominik Steinle[3,6], Lester Barnsley[7], Jie Li[8], Henrich Frielinghaus[5], Dominic Bresser[3,6], Cristina Iojoiu[2,9,*], Elie Paillard[8,*]

[1]Helmholtz-Institute Muenster (IEK 12), Forschungszentrum Juelich GmbH, Münster 48149, Germany.
[2]Univ. Grenoble Alpes, Univ. Savoie Mont Blanc, CNRS, Grenoble INP (Institute of Engineering Univ. Grenoble Alpes), LEPMI, UMR5279, Grenoble 38000, France.
[3]Helmholtz Institute Ulm (HIU), Ulm 89081, Germany.
[4]Key Laboratory of Engineering Dielectric and Applications (Ministry of Education), School of Electrical and Electronic Engineering, Harbin University of Science and Technology, Harbin 150080, Heilongjiang, China.
[5]Juelich Centre for Neutron Science at MLZ, Forschungszentrum Juelich GmbH, Garching 85747, Germany.
[6]Karlsruhe Institute of Technology (KIT), Karlsruhe 76021, Germany.
[7]Australian Synchrotron, The Australian Nuclear Science and Technology Organisation(ANSTO), Clayton 3168, Australia.
[8]Politecnico di Milano, Dept. of Energy, Milan 20156, Italy.
[9]Réseau sur le Stockage Electrochimique de l'Energie (RS2E), CNRS FR3459, Amiens Cedex 80039, France.

[*]**Correspondence to:** Prof. Cristina Iojoiu, Université Grenoble Alpes, LEPMI, Grenoble 38000, France; CNRS, LEPMI, Grenoble 38000, France. E-mail: cristina.iojoiu@lepmi.grenoble-inp.fr; Prof. Elie Paillard, Department of Energy, Politecnico di Milano, Milan 20156, Italy. E-mail: elieelisee.paillard@polimi.it

How to cite this article: Shi J, Nguyen HD, Chen Z, Wang R, Steinle D, Barnsley L, Li J, Frielinghaus H, Bresser D, Iojoiu C, Paillard E. Nanostructured block copolymer single-ion conductors for low-temperature, high-voltage and fast charging lithium-metal batteries. *Energy Mater* 2023;3:300036. https://dx.doi.org/10.20517/energymater.2023.27

Received: 17 Apr 2023 **First Decision:** 8 May 2023 **Revised:** 29 May 2023 **Accepted:** 20 Jun 2023 **Published:** 21 Jul 2023

Academic Editor: Wei Tang **Copy Editor:** Fangyuan Liu **Production Editor:** Fangyuan Liu

Abstract

Herein, a single-ion polymer electrolyte is reported for high-voltage and low-temperature lithium-metal batteries that enables suppressing the growth of dendrites, even at high current densities of 2 mA cm^{-2}. The nanostructured electrolyte was introduced into the cell by mechanically processing the polymer powder via an easily scalable process. Important for the potential application in commercial battery cells is the finding that it does not induce aluminum corrosion at high voltages and leads to low interfacial resistance with lithium metal. These beneficial characteristics, in combination with its high single-ion conductivity and its high anodic stability, allow for the stable cycling of state-of-the-art lithium-ion cathodes, such as NMC_{111} and NMC_{622}, in combination with a lithium metal anode at 20 °C and even 0 °C for several hundred cycles.

Keywords: Polymer electrolyte, single-ion conductor, lithium metal, NMC, battery

INTRODUCTION

Primary lithium-metal batteries (LMBs) provide energy densities far beyond any other electrochemical energy storage device and have been an everyday commodity since the 1970s[1], with energy densities of up to more than 700 Wh kg^{-1}, which remain unmatched by any rechargeable battery. On the other hand, secondary LMBs, despite extensive efforts by electrochemists and material scientists for almost half of a century, were commercialized only in 2004, and they represent today a niche market compared to the dominant lithium (Li)-ion technology that uses a graphite anode instead of lithium metal. The latter, however, is closing the gap between its theoretical and practical energy densities. Thus, the current push for a decarbonized economy calls for a switch from graphite insertion anodes to lithium metal for a tenfold increase in specific capacity enabling longer drive-range electric vehicles (EVs).

LMBs, however, suffer from practical limitations that prevent them from competing with Li-ion batteries. The slow Li-ion transport at room temperature (and below) requires high operation temperatures, and the limited anodic stability of the polyether-based solid polymer electrolytes (SPEs) used implies using low voltage cathodes, which is detrimental to energy density. In fact, their operation temperatures could, in principle, decrease to 40 °C, thanks to strategies to make poly(ethylene oxide) (PEO)-based SPEs amorphous and conductive below the melting point of PEO[2,3]. However, the practical operation temperature of the current generation of commercial lithium-metal polymer batteries (LMPBs) is still above 70 °C, which requires either pre-heating or maintaining the temperature of the battery constantly elevated. Even at these temperatures, though, fast charging is impossible. It is due, on the one hand, to the rapid growth of lithium dendrites that occurs when the current density reaches a diffusion limit at which the lithium salt concentration gradients in the electrolyte are so steep that the lithium concentration at the lithium metal electrode reaches zero[4], which results in fast short-circuits. Additionally, inhomogeneous deposition of lithium usually occurs below this limit, mainly due to the passivation layer at the lithium surface, the so-called "Solid Electrolyte Interphase" (SEI)[5,6]. The SEI might induce an inhomogeneous current density, leading to protrusion of lithium metal and SEI cracking, snowballing to more inhomogeneous deposition and possibly local depletion of lithium that then triggers dendrite growth along local (spherical) salt concentration gradients[7], resulting in the formation of the so-called "mossy lithium" over cycling, which is extremely detrimental for cell performance and safety.

As lithium is a ductile metal, lithium protrusions can be tackled by using polymer electrolytes with sufficient mechanical stability[8] or engineering the interface[9-14] to prevent lithium protrusion (i.e., by mechanical confinement and ensuring homogeneous lithium transport) and the chain of events leading to mossy lithium growth below the limiting current density. However, the fundamental issue of lithium depletion both at high and moderate current rates is directly linked to anionic mobility and diffusion-controlled Li^+ transport. Besides the problematic dendrite growth, diffusion-controlled Li-ion transport means that the electrolyte resistance increases during charge or discharge when the concentration gradients are steep (i.e., the currents are high). Thus, suppressing anion mobility logically results in a decreased internal resistance independent of current, thereby lowering heat generation and energy losses at high currents.

Since the 1990s, single-ion conductors with fixed anions have been proposed to prevent lithium depletion during charge[3,15-18]. Among these, rigid solid-state electrolytes, such as ceramics or glasses, impose finding solutions to buffer not only the large anode volume changes upon cycling but also those more limited cathode materials[19]. On the other hand, Elastomeric polyanions, which are lithium salts where the anionic moieties are linked to a polymer backbone, allow easier processing and buffering electrode volume changes, similar to SPEs that use a lithium salt dissolved in a polymer matrix. The achievement of a true single-ion

conductor, however, also requires preventing polymeric chain reptation, which requires crosslinking. This can be done via classical chemical (covalent) crosslinking, but other strategies have been proposed for obtaining "physical' crosslinking, for instance, using biphasic systems[20-22]. In this case, one "rigid" phase (i.e., crystalline or high Tg) is responsible for the mechanical properties, and the other phase ensures Li^+ transport. This allows decorrelating Li^+ mobility and mechanical properties, both usually linked to polymer chain mobility in monophasic systems. Recently, this approach has been extended to single-ion "dry" SPEs[23,24]. However, one issue arises for phase-separated systems that include a "dry" SPE phase, which is the need, in principle, to include solvating and ionic functions onto the same block while maintaining high chain segmental mobility, similar to "dry" single-ion monophasic SPEs. Thus, in general, polyether chains are used for ensuring solvation and Li^+ mobility, which results in many of the same limitations as for conventional SPEs in terms of electrochemical stability window and operational temperature range. We recently reported on plasticized ionomeric block copolymers with nano-phase separation based on polyaromatic backbones able to operate a Li||$LiNi_{0.33}Mn_{0.33}Co_{0.33}O_2$ (NMC_{111}) battery at 40 °C[25]. Here, we propose a plasticized single-ion SPE for fast-charging and low-temperature Li||NMC_{111} and Li||NMC_{622} high-energy LMPBs. Keeping large-scale production in mind, the electrolyte is obtained here via mechanical processing of the polymer powder incorporating a high dielectric constant liquid phase, which opens the route for high-volume production via extrusion and rapid implementation of the technology.

EXPERIMENTAL SECTION

Synthesis of polyanionic copolymers

The polyanionic copolymers noted as PTFSI-A/B are aromatic polyethersulfone multi-block copolymers with ionic blocks bearing lithium trifluoromethane sulfonimide (TFSI), abbreviated as LiTFSI, and hydrophobic blocks with high glass transition temperatures, i.e., partially fluorinated polysulfone. The A and B are related to the lengths of ionic and hydrophobic block backbones, respectively. In a typical example, i.e., a copolymer named PTFSI-10/5 [Scheme 1], the hydrophobic block with a glass transition temperature (Tg) of 220 °C and a molecular weight of 5,000 g mol^{-1} alternates with the ionic block. The ionic block has a molecular weight of 10, 000 g mol^{-1} in the block backbone and two LiTFSI functions per structural unit. The synthesis of these copolymers, carried out in three steps, i.e., (i) backbone copolymer synthesis by a polycondensation reaction; (ii) bromination of an ionic block; and (iii) grafting of TFSI lithium salt by coupling reaction, was described previously[25-27]. Copolymers with high molecular weight (Mw) are obtained [Supplementary Table 1]. For PTFSI-10/5, the Mw and polydispersity index (Ip) of PTFSI-10/5 are 362, 000 g mol-1 and 2.2, respectively, hence in copolymer chains, the repetition of ionic and hydrophobic blocks (x) ranges between 4 and 10. The lithium concentration in dried membranes, determined from nuclear magnetic resonance (NMR) spectra and acid-base titration (following the protocols described in[25,27]), is presented in Supplementary Table 1. For PTFSI-10/5, the average value is 1.15 10^{-3} mol Li^+ g^{-1}.

Polymer electrolyte processing

The copolymer powder was dried under vacuum at 100 °C for 24 h before use. Propylene carbonate (PC, BASF, Selectipur(TM)) was dried and kept on 4 Å molecular sieves. The polymer electrolytes were prepared in a dry room with a dew point of -65 °C (i.e., H_2O < 5.4 ppm). The copolymers and PC were mixed in various PTFSI/PC weight ratios, and the mixtures were sealed in a laminated "pouch bag" under vacuum and stored at 70 °C for 24 h to ensure good uptake of the liquid phase. The mixture was then sandwiched between two Mylar foils. After pressing at 10 bar for 5 min at room temperature (using another 100-µm Mylar foil as a spacer), self-standing polymer electrolyte membranes were obtained. In the following, the electrolytes are named according to the polymer name, followed by the PC weight fraction in the membranes (e.g., PTFSI-10/5-70 for a SPE containing 70 wt.% of PC).

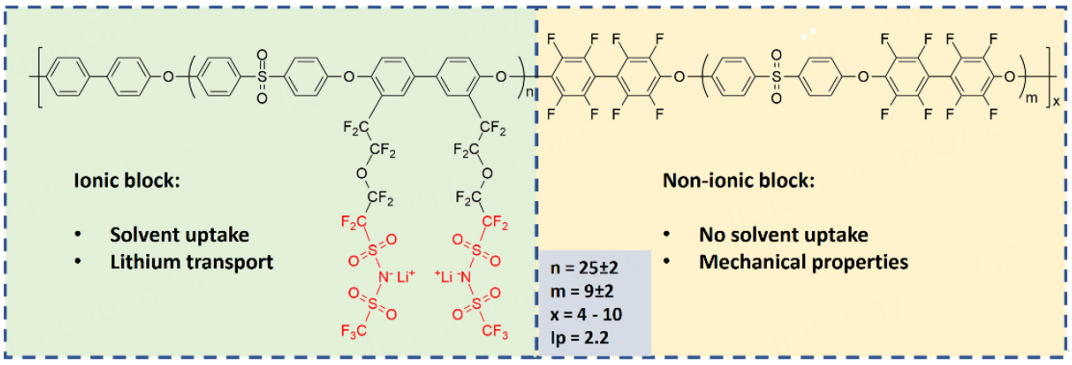

Scheme 1. Schematic representation of PTFSI-10/5.

Conductivity measurements

For conductivity measurements, 2,032 coin cells, including stainless steel (SS) electrodes and the polymer electrolyte membranes, were prepared. The bulk resistance (R_b) of the polymer electrolytes was extracted from the electrochemical impedance spectroscopy (EIS) of the coin cells and determined using a Novocontrol Alpha-A analyzer equipped with a ZG2 extension interface and a cryostat for temperature control in the frequency range of 1 MHz to 1 Hz with a voltage amplitude of 10 mV. The temperature was first ramped from 20 °C to 80 °C and then from 80 °C to -5 °C with 30 min stabilization at each temperature. The conductivity (σ) was calculated according to Equation (1):

$$\sigma = \frac{d}{R_b \times S} \quad (1)$$

where d is the thickness of the polymer electrolyte membranes (100 µm), and S is the area of the electrodes (12 mm diameter).

For measuring the conductivity of the 1M LiTFSI, PC reference liquid electrolyte, a Biologic MSC10 multichannel, EIS-based conductivity meter was used with conductivity cells with a cell constant of *ca.* 1, calibrated prior to each measurement with a standard KCl solution.

Determination of the Li^+ transport number

The Li-ion transport number (t^+) can be calculated using the self-diffusion coefficients of the ionic species in the electrolyte. These coefficients are obtained through pulsed field gradient nuclear magnetic resonance (PFG-NMR) measurements with a Bruker Advance III HD spectrometer equipped with a diffusion probe of 5 mm and a temperature regulation unit. The frequencies are 376.50 and 155.51 MHz for ^{19}F and ^{7}Li, respectively. The maximum magnitude of the pulsed field gradient was 900 $G.cm^{-1}$, the diffusion delay Δ was adjusted between 50 and 100 ms, and the gradient pulse length δ was set between 1 ms and 5 ms. Data acquisition and treatment were performed with Bruker Topspin software. The t^+ was calculated with Equation (2):

$$t^+ = \frac{D_{Li}}{D_{Li} + D_F} \quad (2)$$

where D_{Li} is the self-diffusion coefficient of the Li^+, and D_F is the self-diffusion coefficient of the anion[28].

Small-angle neutron scattering

Small-angle neutron scattering (SANS) measurements were performed on the small-angle diffractometer KWS-1 operated by the Forschungszentrum Juelich at the Heinz Maier-Leibnitz Zentrum in Garching/Munich to identify the phase structure of the polymer electrolytes. The selected wavelength was 0.45 nm, and the detector distances were 2 and 8 m, with the collimation being 8 m. The electrolyte membranes containing PTFSI copolymers with various block lengths and PC contents were prepared with a thickness of ~100 μm and diameter of 12 mm and were sealed in pouch bags (5 cm × 5 cm) under vacuum in the dry room. An empty pouch bag and a pouch bag with 1 mL of PC of the same size were prepared as references.

Electrochemical characterization

Symmetric Li‖Li cells were assembled to investigate the lithium electrode cycling behavior. 330 μm Li foils (Rockwood Lithium) were used in combination with either 1M LiTFSI in PC comprised in a Whatman GF/D glass fiber separator or with the PTFSI-10/5-70 membranes. A current density of 2 mA cm^{-2} was applied and reversed every 30 min. Electrochemical impedance spectra were acquired on a VMP3 potentiostat (Biologic) to track the changes of the impedance of Li‖Li cells during the cycling process using a 10 mV amplitude. To characterize the morphology of the plating for high plating capacity, similar symmetrical cells were assembled, and a current of 1 mA cm^{-2} was applied for 10 h. The cells were then disassembled in a glovebox under argon with H_2O and O_2 levels below 1 ppm, and the samples were transferred to the scanning electron microscope (SEM) chamber (Zeiss Auriga) without air exposure using a hermetical cell. SEM images of the plated lithium metal electrode were then acquired.

For the study of the Al current collector corrosion, cyclic voltammetry (CV) was performed on a VMP3 potentiostat (Biologic) with Li‖Al two-electrode coin cells between 3.0 and 5.0 V. The sweep rate was 1 mV s^{-1}. For the battery tests, $LiNi_{0.33}Mn_{0.33}Co_{0.33}O_2$ (NMC_{111}) electrodes were prepared by mixing NMC_{111} (Toda), Super C65 (Inerys), PVdF (Solvay, Solef 5130), and PTFSI-10/5 in the ratio 8:1:0.75:0.25 by weight. $LiNi_{0.6}Mn_{0.2}Co_{0.2}O_2$ (NMC_{622}) electrodes were prepared by mixing NMC_{622} (Rongbai), Super C65 (C-NERGY), and PVdF (Solvay, 6020) with a weight ratio of 9.2:0.4:0.4. The mass loading of NMC was ~2.4 mg cm^{-2}. The $LiFePO_4$ (LFP) electrodes were prepared similarly to the NMC electrode with LFP: Super C65: PVDF: PTFSI-10/5= 8:1:0.75:0.25 by weight. The mass loading of LFP was ~1.41 mg cm^{-2}. The cells were first cycled at 0.1 C for three cycles and then at different dis-/charge rates.

RESULTS AND DISCUSSION

Polymer electrolyte processing and characterization

More often than not, block copolymers designed for nano-phase separation require a careful selection of the solvent for casting membranes with a well-defined phase separation upon solvent removal. We showed previously, for a similar polymer with longer blocks and a higher fraction of "rigid phase" (PTFSI-15/15), that the solvent used to cast the dry membrane affects the phase separation. Specifically, we found that dimethyl sulfoxide (DMSO) allows for a sharp hydrophobic-ionic phase separation and a more regular phase structure as compared with dimethylacetamide (DMAc). Nevertheless, in both cases, SANS measurements unambiguously revealed a clear phase separation and a constant non-ionic domain size upon ethylene carbonate (EC) uptake[25]. The hydrophobic block, i.e., partially fluorinated copolymer, was designed to be non-miscible with high dielectric constant solvents, such as EC and PC. However, solvent casting, followed by the removal of a high boiling point solvent, such as DMSO or DMAc, and the dry membrane swollen by the suitable solvent(s), is a lengthy and energy-consuming process, thus *a priori* too costly for a future scale-up of such technology. Therefore, in the current study, we processed the electrolytes using solely the eventually comprised liquid phase (i.e., PC) and the polymer powder. A mixing step at a moderate temperature (70 °C) was followed by a pressing step in a laboratory-scale process mimicking the

extrusion of a membrane with the liquid phase. PC was used instead of EC to avoid any crystallization down to the melting point of PC (-48.5 °C), even at high solvent contents. In fact, herein, a PC content of up to 70 wt% was used in combination with a polymer with shorter hydrophobic blocks than previously reported (5,000 *vs.* 15,000 M_w) for improving the polymer electrolyte processability.

SANS measurements were performed to assess the phase separation. The results are shown in Figure 1A for the PTFSI-based polymer with 30 wt% of PC with increasing ionic block length: PTFSI-5/5-30 [i.e., with ionomeric and (respectively) non-ionic blocks of 5,000 g mol^{-1} and 30 wt% PC], PTFSI-10/5-30, and PTFSI-15/5-30 to compare the different block copolymers. On the other hand, the effect of increasing solvent fractions is shown for PTFSI-10/5. The phase separation is overall less marked than what was obtained with DMSO-cast membranes but similar to EC-membranes obtained using DMAc as the casting solvent. The comparison of the different polymers shows that the PTFSI-15/5-30 phase separation is less marked than for the membranes with shorter ionic blocks (PTFSI-5/5-30 and PTFSI-10/5-30). The phase separation of the PTFSI-10/5 electrolytes is well maintained with increasing PC content, and all electrolytes exhibit a hydrophobic domain size of 13 nm.

The conductivity of the PTFSI-10/5-70 electrolyte shown in Figure 1B is *ca.* ten times lower than that of the liquid reference (1M LiTFSI in PC). It must be noted, however, that the liquid electrolyte requires the use of a separator to be used in battery cells that would induce a decrease by a factor of 10 of the conductance of the (electrolyte + separator) assembly[29]. Besides, the conductivity is linked to anions and cations for the liquid electrolyte. Probably due to poorer phase separation of hydrophobic domains and thus a more tortuous ionic pathway, in this case, the ionic conductivities are somewhat lower than those previously reported for EC-plasticized membranes obtained via DMSO casting and subsequent swelling. The PTFSI-10/5-70 membrane, however, still reaches 2.15×10^{-4} S cm^{-1} at 20 °C and 8.98×10^{-5} S cm^{-1} at 0 °C, which, for a single-ion conductor that is able to maintain a fast lithium transport at steady-state is, in principle, sufficient for the application[30].

In fact, even the electrolyte with the highest PC content (PTFSI-10/5-70) exhibits a t^+ of 1 as no diffusion was detected for the anionic moiety, even at 90 °C (see Table 1). A Li^+ self-diffusion coefficient of 0.31×10^{-10} m^2 s^{-1} was determined at 30 °C, which is more than 50 times higher than a reinforced PEO/ionic liquid (IL)/LiTFSI plasticized polymer electrolytes (0.6×10^{-12} m^2 s^{-1} at 25 °C[31]). Moreover, it is similar, at 70 °C, to what was measured for a PTFSI-15/15 polymer with 30 wt% of EC obtained using a DMSO cast membrane (0.95 *vs.* 0.96×10^{-10} m^2 s^{-1}).

With a lithium content of 1.15×10^{-3} mol g^{-1} in the dry PTFSI-10/5 polymer, if we postulate a density of 1.2 for the final electrolyte, the lithium content in the plasticized electrolyte corresponds to *ca.* 0.29 mol L^{-1}. This is relatively low compared to the most conductive concentrations in most organic lithium conducting electrolytes [e.g., PEO/IL/LiTFSI (plasticized or not) electrolytes or LiTFSI in PC]. Hence, it is likely that increasing the grafted lithium salt concentration would lead to improved conductivity as an effect of increased charge carrier concentration. Noticeably, the PTFSI-10/5-50 electrolyte exhibits a conductivity close to that of the PTFSI-10/5-70 electrolyte at high temperatures, indicating that the higher charge density, resulting from the lower PC content, is favorable at higher temperatures (where ionic mobility is higher). If we calculate the theoretical conductivity from the Nernst-Einstein equation (Equation 3) and D_{Li}, we reach a molar conductivity of 1.14 S cm^2 mol^{-1} and a Li^+ conductivity of 3.3×10^{-4} S cm^{-1} at 30 °C, which is only 12% higher than the experimentally determined value of 2.9×10^{4} S cm^{-1}. This is in excellent agreement with single-ion conductivity and indicates that the ionic functions are well dissociated. The small difference can be easily accounted for (besides the experimental errors and the hypothesis on density) by the presence of the non-conductive phase.

Table 1. Self-diffusion coefficients at different temperatures derived from PFG-NMR measurements and lithium transport numbers calculated via Equation (1) for the PTFSI-10/5-70 electrolyte

T (°C)	D_{Li} (10^{-10} m^2 s^{-1})	D_F (10^{-10} m^2 s^{-1})	t^+
30	0.31 ± 0.01	No measurable diffusion	1
50	0.57 ± 0.02	No measurable diffusion	1
70	0.95 ± 0.03	No measurable diffusion	1
90	1.49 ± 0.04	No measurable diffusion	1

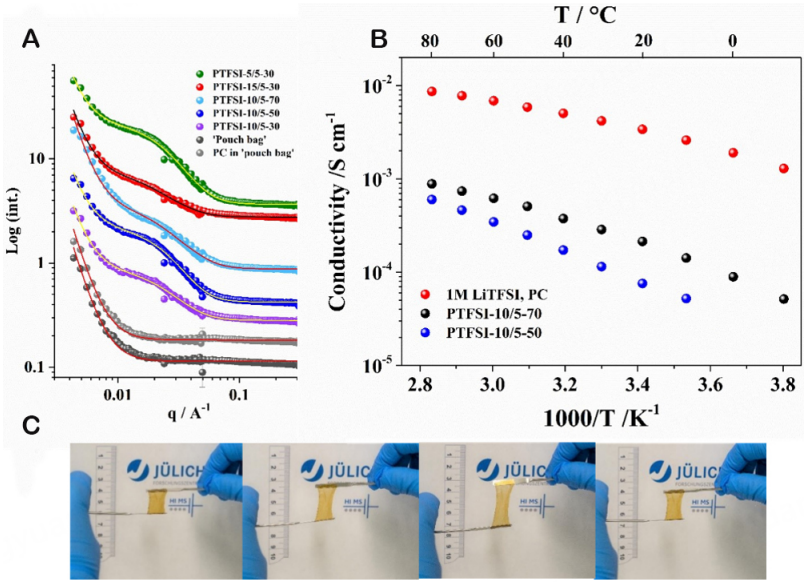

Figure 1. (A) SANS spectra of various single-ion polymer electrolytes and reference cells. (B) Conductivity of PTFSI-10/5-50, PTFSI-10/5-70, and 1M LiTFSI, PC. (C) Illustration of the elastic behavior of the PTFSI-10/5-70 electrolyte.

$$\Lambda_e = \frac{z_i^2 * F^2}{RT}(D^+ + D^-) \quad (3)$$

With Λ_e the molar conductivity (S cm^2 mol^{-1}), F the Faraday constant (96,485 C mol^{-1}), R the gas constant (8.31 J mol^{-1} K^{-1}), T the temperature (K), and D^+ and D^- the diffusion coefficients (cm^2 s^{-1}) of the Li^+ and anions.

The electrochemical stability window shown in Supplementary Figure 1 is rather wide, with only a very low background current prior to lithium deposition in the cathodic scan, and the stability toward oxidation is seemingly higher than that of the 1M LiTFSI in the PC electrolyte and similar to that of the EC-plasticized membranes[25]. A small peak around 4.5 V can be observed, as previously reported for PTFSI-15/15 with 50 wt% of EC. It likely originates from alkyl carbonate decomposition since a similar peak is also observed for 1M LiTFSI in PC. The appearance of the PTFSI-10/5-70 used in the following is shown in Figure 1C.

Lithium metal electrode cycling and high-voltage lithium cells

The operation of the lithium metal anode is not only dependent on the electrolyte bulk transport properties but also on the formation of a favorable SEI layer at the interface between lithium metal and electrolyte. On

the one hand, the cell assembly process should not induce inhomogeneity for lithium transport pathways, and the "softness" of the PTFSI-10/5-70 electrolyte is favorable in this regard. Indeed, hard contact points would be likely to induce cracks in the passivation layer already present on the lithium foil following its production by extrusion in dry air or Ar/CO_2 and result in inhomogeneous lithium transport. On the other hand, the resistance of the SEI should allow fast lithium transport and not be the limiting factor. In fact, it is known from IL-electrolytes[32] or ternary IL-plasticized polymer electrolytes[33] that the SEI resistance often represents a much higher hindrance to Li^+ transport than that of the IL-free electrolyte, especially at ambient and sub-ambient temperature.

Figure 2A compares the voltage profiles of symmetrical Li||Li cells using either the liquid reference electrolyte (1M LiTFSI in PC) within a thick glass fiber separator or a PTFSI-10/5-70 membrane. As can be seen, with the liquid reference electrolyte, the overvoltage first decreases as the surface area of lithium increases but then continuously increases. This can be explained by the formation of mossy lithium during plating that leaves behind, upon lithium stripping, electronically disconnected lithium residues mixed with electrolyte reduction products, which ends up forming a mixed layer that slows down Li-ion transport[34]. When analyzing the voltage profiles shown in more detail (see the inserts), one can see, at the beginning of each step and after the immediate polarization of the cell, an asymptotic exponential increase to a steady-state voltage as concentration gradients are getting established, thereby increasing the electrolyte resistance. The corresponding impedance spectra [Figure 2B] reveal that the impedance of the cell strongly evolves upon cycling. In the beginning, only one well-defined semi-circle corresponding to the SEI resistance is observed that decreases accordingly with the increase of surface area upon initial plating/stripping. However, it is compensated by the appearance of a second flattened semi-circle at lower frequencies and even a third one after longer cycling. This can tentatively be attributed to the plating and stripping of mossy lithium and the formation of a thick layer, at a larger scale, unfavorable for Li-ion transport. In fact, Figure 2D shows the aspect of a lithium metal electrode after a single lithium plating of 10 mAh cm^{-2} at 1 mA cm^{-2} using the same cell configuration, revealing the presence of dendrites on the plated electrode (some of the dendrites were trapped in the separator and removed upon cell disassembly).

On the other hand, the voltage profiles of the cells using a PTFSI-10/5-70 membrane as electrolyte have a square shape, with no evidence of internal resistance change during any step, neither at the beginning nor at the end of the cycling, which confirms that lithium transport is time-independent due to the single-ion conduction. Over cycling, the overvoltage is essentially constant, with, however, a small decrease over cycling that can be attributed to a slight increase in lithium surface area. Indeed, even though single-ion conduction prevents "top grown" dendrites, SEI inhomogeneities might still induce an increase of surface area. In fact, after the plating of 10 mAh cm^{-2} of Li (i.e., roughly 50 μm) at 1 mA cm^{-2}, it can be seen from Figure 2E that the deposited Li is not fully flat, although there is no evidence of dendrites. In line with this, the evolution of impedance spectra reveals that the resistance of the electrolyte is much lower (due to a much thinner electrolyte, *ca.* 100 μm) and that the SEI resistance (corresponding roughly to the diameter of the semi-circle) is quite constant over cycling [Figure 2C]. A minimal decrease in resistance can be attributed to the slight increase of surface area but in a much lower proportion compared to that of the liquid electrolyte since no dendrite is formed in the former case. The SEI resistance is also very low, which is an additional feature of this electrolyte and can tentatively be attributed to the high fluorine content of the polymer, favorable for forming a thin and protective SEI and the limited polymer and anion degradation due to their immobility[35].

These current rates are very high for LMPBs (which typically include lower mass loading per surface area to compensate for low current densities) and especially remarkable, considering that the lithium metal used is

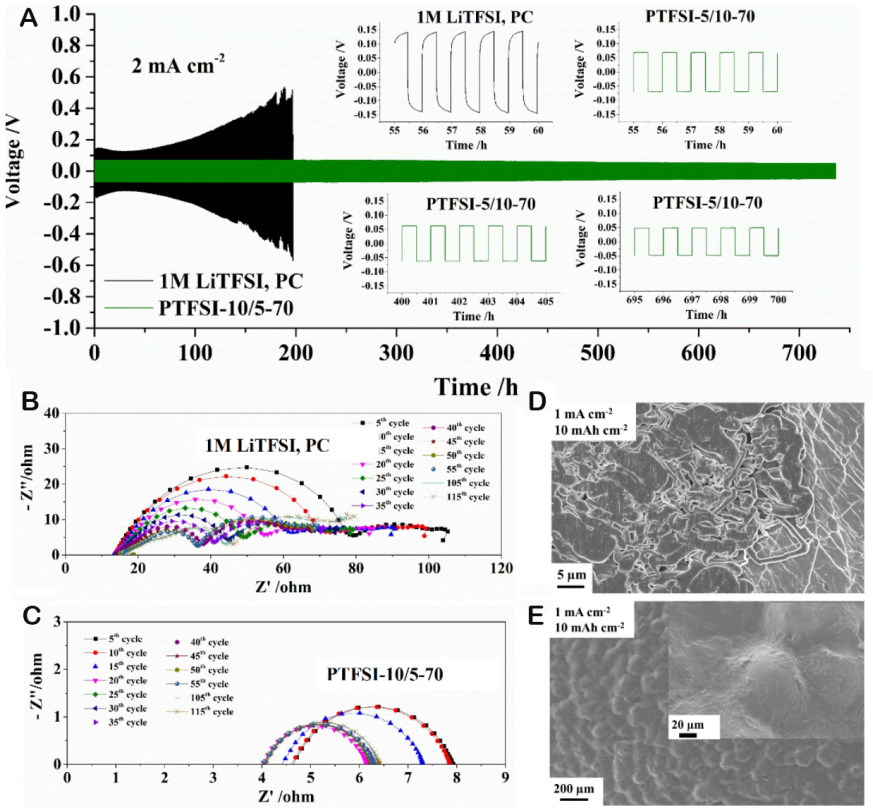

Figure 2. (A) Voltage profiles of Li/Li symmetrical cells using either 1 M LiTFSI in PC (+ Whatman GF/D as separator) or PTFSI-5/10-70 as an electrolyte at 20 °C. Current density: 2 mA cm^{-2} reversed every 30 min (i.e., 1 mAh cm^{-2} cycled at 2C). (B) Impedance spectra acquired every five cycles for a 1M LiTFSI, PC Li/Li cell cycled at 2 mA cm^{-2}. (C) Impedance spectra acquired every five cycles for a PTFSI-5/10-70 Li/Li cell' cycled at 2 mA cm^{-2}. (D) SEM image of a lithium electrode after plating 10 mAh cm^{-2} at 1 mA cm^{-2} at 20 °C in 1M LiTFSI, PC (+ Whatman GF/D separator). (E) SEM images of a lithium electrode covered by PTFSI-4/10-70 after plating 10 mAh cm^{-2} at 1 mA cm^{-2} at 20 °C using PTFSI-5/10-70 as the electrolyte.

a regular lithium foil kept in a glovebox and that further improvement could be enabled by tuning the pressure applied and by lithium/electrolyte interface optimization since fully homogenous plating of lithium metal is a multi-parameter issue.

To demonstrate the applicability of the electrolyte membrane for high-voltage and high-energy lithium metal cells, several cathode materials have been tested at 20 °C. LFP is the state-of-the-art for LMPBs and showed excellent cycling behavior at 20 °C [Supplementary Figure 2]. Since the main target of switching from PEO-based electrolytes is the achievement of high-voltage lithium metal cells that are able to operate at ambient and sub-ambient temperatures, NMC cathodes have been studied as well. Figure 3 shows the cycling performance obtained at various current densities with NMC_{111} cathodes. The current densities are calculated, in this case, based on the lithium metal surface area. The capacity decays relatively fast with increasing current densities compared to what was expected from the Li|Li cells. It likely results from the cathode preparation, which has not been optimized yet. Indeed, even though some PTFSI-10/5 was incorporated into the NMC_{111} electrodes to favor ionic contact with the electrolyte membranes, the electrodes used are still porous, whereas an optimized cell would use dense electrodes instead (i.e., have all the porosity filled with polymer electrolyte). Nevertheless, cycling is possible using various current densities of up to 1 mA cm^{-2}. If we consider a typical Li-ion battery mass loading of *ca.* 2 mAh cm^{-2} (i.e., typical for a PHEV2 battery cell for plug-in hybrids), the current densities of 0.25, 0.5, and 1 mA cm^{-2} would correspond

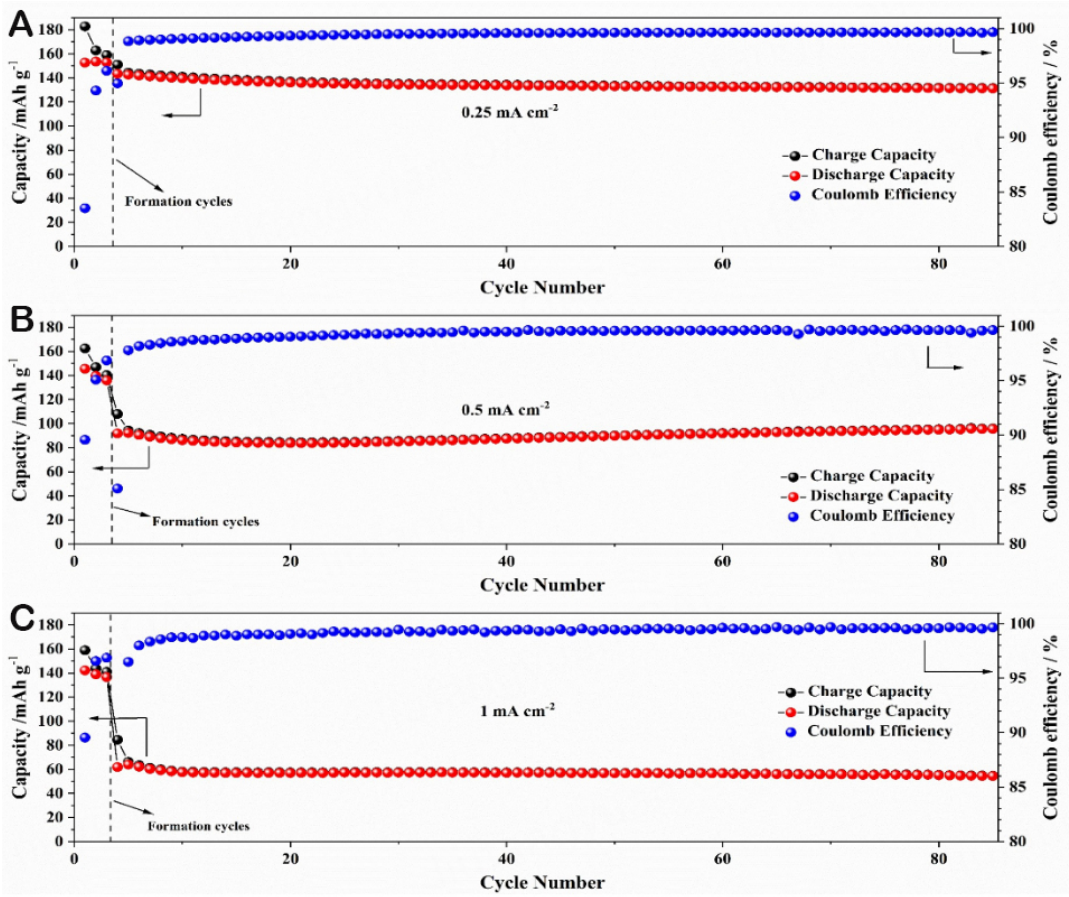

Figure 3. Cycling of Li/NMC111 cells at 20 °C. (A) 0.25 mA cm^{-2}, (B) 0.5 mA cm^{-2}, and (C) 1 mA cm^{-2}.

to C/8, C/4, and 1C, respectively. As can be seen, the cycling is very stable at all of these current densities. Long-term cycling (up to 500 cycles) was possible and is shown for the two higher current rates in Supplementary Figure 3.

The state-of-the-art for automotive applications has shifted from NMC_{111} to NMC_{622}, which is, at the same time, less costly in terms of raw materials, less toxic, and more ethical considerations. NMC_{622} achieves these benefits by incorporating the lower Co content while providing higher energy densities. Thus, we also constructed Li‖NMC_{622} cells and their behavior at 20 °C, as shown in Figure 4A and B. The rate performance is good up to C/2 with capacities above 120 mAh g^{-1}, and most importantly, for lithium metal cells, the relatively high rates used for the rate test do not induce any decay of performance upon returning to C/2. Li‖NMC_{622} cells were also cycled at 0 °C, as shown in Figure 4C and D. The rate performance obviously decays with temperature, but high capacities are still reachable at low rates (*ca.* 80 mAh g^{-1} at C/2). Long-term stable cycling for more than 300 cycles was also obtained at both 20 °C and 0 °C after the rate test [Supplementary Figure 4]. This is even more remarkable since elevated dis-/charge rates usually have a strong detrimental effect on the long-term cycling performance of lithium metal cells when using electrolytes that do not prevent dendrite growth.

Since the electrolyte membrane contains PC, the electrolyte is still flammable, although PC exhibits a much lower vapor pressure (0.2936 kPa at 25 °C[36]) than the linear alkyl carbonates commonly used in Li-ion

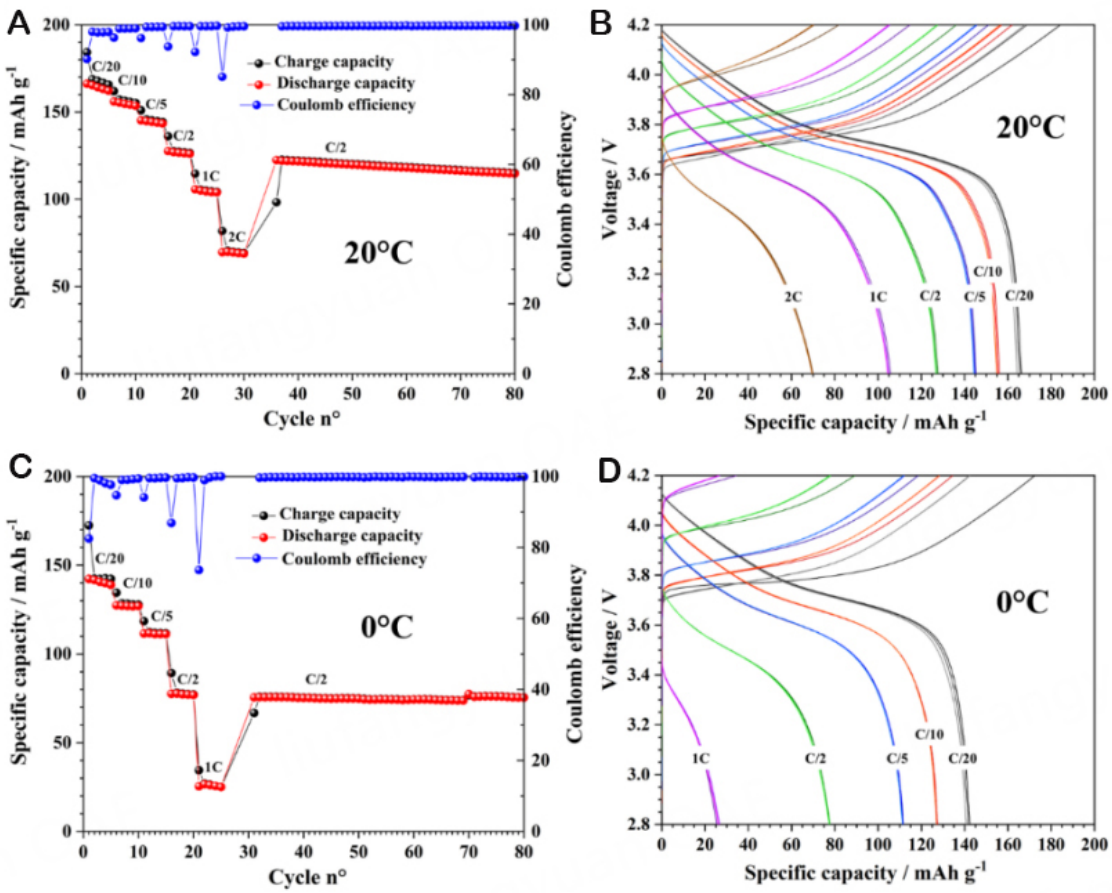

Figure 4. (A) Rate capability test of a Li/NMC622 cell at 20 °C, (B) Corresponding voltage profiles, (C) Rate capability test of a Li/NMC622 cell at 0 °C, (D) Corresponding voltage profiles.

electrolytes. PC also exhibits a high flash point (F_p) of 132 °C (*vs.* < 30 °C for dimethyl carbonate, diethyl carbonate, and ethyl methyl carbonate commonly used in most Li-ion batteries electrolytes). Nevertheless, the polymer can also be used with very high boiling points and low vapor pressure solvents such as adiponitrile (Bp = 295.1 °C, vapor pressure = 300 mPa at 20 °C) that also allows cycling Li‖NMC_{111} cells at 20 °C, as shown in Supplementary Figure 5, although the use of a dinitrile solvent results in a likely degraded Li/electrolyte interface, as seen with the decay of efficiency after *ca.* 60 cycles.

Investigation of the aluminum corrosion

Since the electrolyte comprises pending anionic moieties that have a chemical structure similar to the TFSI anion and given the fact that LiTFSI is known to induce corrosion of the Al cathode current collector above 4 V, it is important to evaluate the behavior of the polymer electrolyte toward Al at high voltage for the application.

Figure 5 provides a comparison of the Al corrosion behavior of the polymer electrolyte membrane and the liquid reference electrolyte based on 1M LiTFSI. In the case of the single-ion polymer electrolyte, a very low anodic current is observed in the first cycle (< 5 μA cm^{-2}, insert in Figure 5A), with a slight increase above 4.5 V, especially during the first scan. Nonetheless, even at this high voltage, the evolving current density remains below 1 μA cm^{-2}. In sharp contrast, the liquid reference electrolyte containing LiTFSI induces strong Al corrosion, resulting in evolving current densities exceeding 2 mA cm^{-2}. Representative

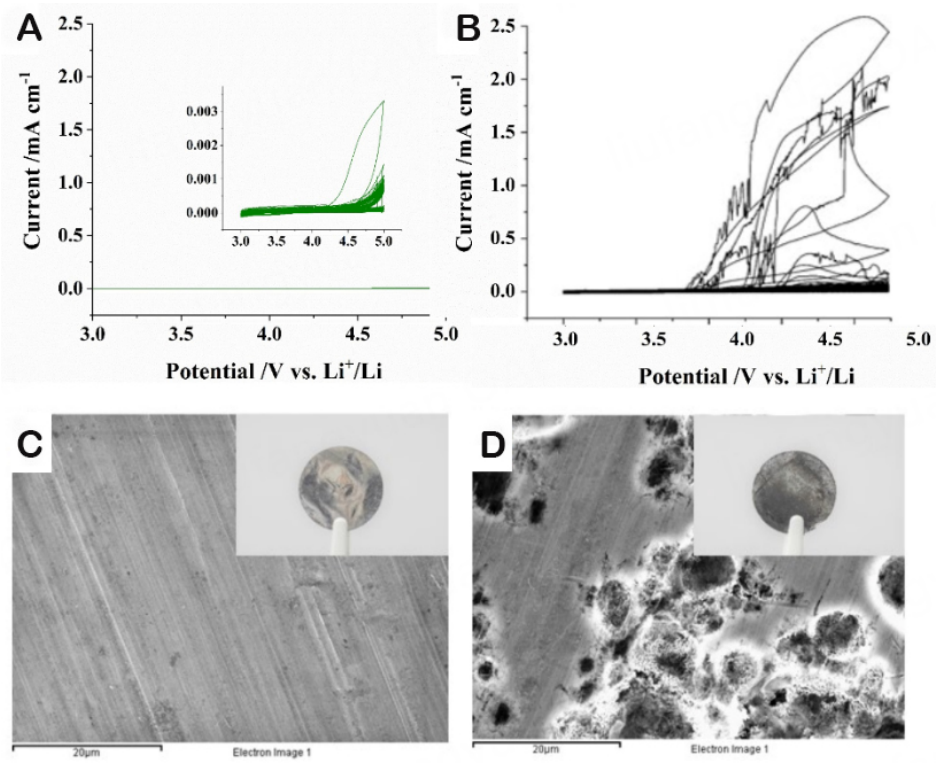

Figure 5. Voltammograms profiles of Li/Al cells using (A) PTFSI-5/10-70 or (B) 1 M LiTFSI in PC (+ Whatman GF/D as separator) as electrolyte at 23 °C. SEM images of the Al electrodes after the tests with (C) PTFSI-5/10-70 and (D)1 M LiTFSI in PC (+ Whatman GF/D as separator).

photographs and SEM images are presented in Figure 5C and D, confirming the absence of Al corrosion in the case of the polymer electrolyte and the severe Al corrosion in the case of the liquid reference electrolyte, respectively.

CONCLUSIONS

The electrolyte PTFSI-10/5-70 allows for overcoming many issues that are limiting the penetration of LMPBs into the booming market of EVs. In particular, it tackles the low operation temperature issues of such devices, decreasing their potential operation to sub-ambient temperatures as low as 0 °C. Its high anodic stability enables the use of NMC cathodes rather than LFP and, thus, higher energy densities. Most importantly, it allows reaching high lithium plating current densities of 2 mA cm^{-2} with lithium metal due to its single-ion conductivity (despite a rather low charge density that leaves room for further improvements) combined with favorable interfacial properties with lithium metal. This opens the route, combined with future optimized cathodes, to fast-charging LMBs. It is especially promising as the polymer electrolyte was obtained following a straightforward process based on mechanical mixing of the components and pressing, which can be easily translated into high-volume industrial production, for instance, by extrusion. Finally, since the dendrite growth is fully prevented and high currents are possible, this electrolyte will allow removing the dendrite from the equation for addressing the protrusion of lithium metal, which requires full control of the lithium metal interface in terms of homogeneity of current densities and mechanical properties.

DECLARATIONS

Authors' contributions

Prepared the polymer membranes and NMC_{111} cathodes and performed most of the electrochemical experiments with NMC_{111}, Li|Al, and Li|Li cells: Shi J
Synthesized the polymers: Nguyen HD
Performed the SANS measurements: Wang R, Barnsley L, Frielinghaus H
Performed the work on NMC_{622}: Chen Z, Steinle D, Bresser D
Designed the polymer concept and performed the PFG-NMR measurements: Iojoiu C
Supervised the project: Paillard E, Iojoiu C
Analyzed the data and co-wrote and discussed the whole paper: Shi J, Nguyen HD, Chen Z, Wang R, Steinle D, Barnsley L, Li J, Frielinghaus H, Bresser D, Iojoiu C, Paillard E

Financial Support and Sponsorship

The authors would like to acknowledge the financial support from the French National Research Agency within the NSPEM project (ANR-16-CE05-0016), the Center of Excellence of Multifunctional Architectured Materials "CEMAM" (AN-10-LABX-44-01), the support of the European Commission within the H2020 Project VIDICAT (GA n° 829145), as well as the Federal Ministry for Education and Research (BMBF) for financial support within the FestBatt (03XP0175B), the FB2-Poly (03XP0429B), and the LISI (03XP0224D) projects.

Availability of Data and Materials

The data are made available upon request to authors.

Conflicts of Interest

All authors declared that there are no conflicts of interest.

Ethical Approval and Consent to Participate

Not applicable.

Consent for Publication

Not applicable.

REFERENCES

1. Colin AV. Lithium batteries: a 50-year perspective, 1959–2009. *Solid State Ion* 2000;134:124-9. DOI
2. Zaghib K, Charest P, Guerfi A, Shim J, Perrier M, Striebel K. Safe Li-ion polymer batteries for HEV applications. *J Power Sources* 2004;134:159-67. DOI
3. Iojoiu C, Paillard E. Solid-state batteries with polymer electrolytes. In: Bard AJ, editor. Encyclopedia of Electrochemistry. Wiley; 2007. pp. 1-49. DOI
4. Chazalviel J. Electrochemical aspects of the generation of ramified metallic electrodeposits. *Phys Rev A* 1990;42:7355-67. DOI PubMed
5. Peled E. The electrochemical behavior of alkali and alkaline earth metals in nonaqueous battery systems—the solid electrolyte interphase model. *J Electrochem Soc* 1979;126:2047-51. DOI
6. Peled E, Menkin S. Review-SEI: past, present and future. *J Electrochem Soc* 2017;164:A1703-19. DOI
7. Rosso M, Gobron T, Brissot C, Chazalviel J, Lascaud S. Onset of dendritic growth in lithium/polymer cells. *J Power Sources* 2001;97-98:804-6. DOI
8. Barai P, Higa K, Srinivasan V. Lithium dendrite growth mechanisms in polymer electrolytes and prevention strategies. *Phys Chem Chem Phys* 2017;19:20493-505. DOI
9. Cao X, Ren X, Zou L, et al. Monolithic solid-electrolyte interphases formed in fluorinated orthoformate-based electrolytes minimize Li

depletion and pulverization. *Nat Energy* 2019;4:796-805. DOI

10. Grande L, von Zamory J, Koch SL, Kalhoff J, Paillard E, Passerini S. Homogeneous lithium electrodeposition with pyrrolidinium-based ionic liquid electrolytes. *ACS Appl Mater Inter* 2015;7:5950-8. DOI PubMed
11. Qian J, Henderson WA, Xu W, et al. High rate and stable cycling of lithium metal anode. *Nat Commun* 2015;6:6362. DOI PubMed PMC
12. Qian J, Adams BD, Zheng J, et al. Anode-free rechargeable lithium metal batteries. *Adv Funct Mater* 2016;26:7094-102. DOI
13. Qian J, Xu W, Bhattacharya P, et al. Dendrite-free Li deposition using trace-amounts of water as an electrolyte additive. *Nano Energy* 2015;15:135-44. DOI
14. Zheng G, Lee SW, Liang Z, et al. Interconnected hollow carbon nanospheres for stable lithium metal anodes. *Nat Nanotechnol* 2014;9:618-23. DOI
15. Ohno H, Ito K. Poly(ethylene oxide)s having carboxylate groups on the chain end. *Polymer* 1995;36:891-3. DOI
16. Zhang H, Li C, Piszcz M, et al. Single lithium-ion conducting solid polymer electrolytes: advances and perspectives. *Chem Soc Rev* 2017;46:797-815. DOI
17. Bannister D, Davies G, Ward I, Mcintyre J. Ionic conductivities for poly(ethylene oxide) complexes with lithium salts of monobasic and dibasic acids and blends of poly(ethylene oxide) with lithium salts of anionic polymers. *Polymer* 1984;25:1291-6. DOI
18. Jiang C, Li H, Wang C. Recent progress in solid-state electrolytes for alkali-ion batteries. *Sci Bull* 2017;62:1473-90. DOI
19. Strauss F, de Biasi L, Kim A, et al. Rational design of quasi-zero-strain NCM cathode materials for minimizing volume change effects in all-solid-state batteries. *ACS Mater Lett* 2020;2:84-8. DOI
20. Ruzette AG, Soo PP, Sadoway DR, Mayes AM. Melt-formable block copolymer electrolytes for lithium rechargeable batteries. *J Electrochem Soc* 2001;148:A537. DOI
21. Soo PP, Huang B, Jang Y, Chiang Y, Sadoway DR, Mayes AM. Rubbery block copolymer electrolytes for solid-state rechargeable lithium batteries. *J Electrochem Soc* 1999;146:32-7. DOI
22. Miller TF, Wang ZG, Coates GW, Balsara NP. Designing polymer electrolytes for safe and high capacity rechargeable lithium batteries. *ACC Chem Res* 2017;50:590-3. DOI PubMed
23. Inceoglu S, Rojas AA, Devaux D, Chen XC, Stone GM, Balsara NP. Morphology-conductivity relationship of single-ion-conducting block copolymer electrolytes for lithium batteries. *ACS Macro Lett* 2014;3:510-4. DOI PubMed
24. Bouchet R, Maria S, Meziane R, et al. Single-ion BAB triblock copolymers as highly efficient electrolytes for lithium-metal batteries. *Nat Mater* 2013;12:452-7. DOI
25. Nguyen H, Kim G, Shi J, et al. Nanostructured multi-block copolymer single-ion conductors for safer high-performance lithium batteries. *Energy Environ Sci* 2018;11:3298-309. DOI
26. Assumma L, Iojoiu C, Mercier R, Lyonnard S, Nguyen HD, Planes E. Synthesis of partially fluorinated poly(arylene ether sulfone) multiblock copolymers bearing perfluorosulfonic functions. *J Polym Sci Part A Polym Chem* 2015;53:1941-56. DOI
27. Nguyen HD, Assumma L, Judeinstein P, et al. Controlling microstructure-transport interplay in highly phase-separated perfluorosulfonated aromatic multiblock ionomers via molecular architecture design. *ACS Appl Mater Inter* 2017;9:1671-83. DOI
28. Gorecki W, Andreani R, Berthier C, et al. NMR, DSC, and conductivity study of a poly(ethylene oxide) complex electrolyte: $PEO(LiClO_4)_x$. *Solid State Ion* 1986;18-19:295-9. DOI
29. Landesfeind J, Hattendorff J, Ehrl A, Wall WA, Gasteiger HA. Tortuosity determination of battery electrodes and separators by impedance spectroscopy. *J Electrochem Soc* 2016;163:A1373-87. DOI
30. Thomas KE, Sloop SE, Kerr JB, Newman J. Comparison of lithium-polymer cell performance with unity and nonunity transference numbers. *J Power Sources* 2000;89:132-8. DOI
31. González F, Tiemblo P, García N, et al. High performance polymer/ionic liquid thermoplastic solid electrolyte prepared by solvent free processing for solid state lithium metal batteries. *Membranes* 2018;8:55. DOI PubMed PMC
32. Grande L, Paillard E, Kim GT, Monaco S, Passerini S. Ionic liquid electrolytes for Li-air batteries: lithium metal cycling. *Int J Mol Sci* 2014;15:8122-37. DOI PubMed PMC
33. Kim G, Appetecchi G, Carewska M, et al. UV cross-linked, lithium-conducting ternary polymer electrolytes containing ionic liquids. *J Power Sources* 2010;195:6130-7. DOI
34. Cheng J, Assegie AA, Huang C, et al. Visualization of lithium plating and stripping via *in operando* transmission X-ray microscopy. *J Phys Chem C* 2017;121:7761-6. DOI
35. Yang C, Chen J, Qing T, et al. 4.0 V aqueous Li-ion batteries. *Joule* 2017;1:122-32. DOI
36. Nasirzadeh K, Neueder R, Kunz W. Vapor pressures of propylene carbonate and *N*, *N*-dimethylacetamide. *J Chem Eng Data* 2005;50:26-8. DOI